Structure and Bonding in As−Sb−S Chalcogenide Glasses by Infrared Reflectance Spectroscopy

E. I. Kamitsos* and J. A. Kapoutsis

Theoretical and Physical Chemistry Institute, National Hellenic Research Foundation, 48 Vass. Constantinou Avenue, Athens 116 35, Greece

I. P. Culeac and M. S. Iovu

Center of Optoelectronics, Institute of Applied Physics, nr. 1 Academiei Str., Chisinau, MD-2028, Republic of Moldova

Received: July 17, 1997; In Final Form: September 23, 1997[⊗]

The structure of chalcogenide glasses $x\mathrm{Sb_2S_3}\cdot(1-x)\mathrm{As_2S_3}$ with $0 \le x \le 0.75$ was studied by infrared reflectance spectroscopy. The absorption coefficient spectra, calculated from reflectance by Kramers−Kronig analysis, were deconvoluted in the high-frequency region from 250 to 450 $\mathrm{cm^{-1}}$, and the frequency and relative intensity of the component bands were studied as a function of $\mathrm{Sb_2S_3}$ content. Band assignments were based on the molecular model, and experimental relative intensities were compared with those calculated in terms of the random substitution and heterogeneous structure models proposed in the literature for such glasses. The results were found to be consistent with a glass structure formed by a random distribution of trigonal $\mathrm{AsS_{3/2}}$ and $\mathrm{SbS_{3/2}}$ pyramidal units bridged by sulfur atoms. A band resolved at ca. 360 $\mathrm{cm^{-1}}$ was associated with mixed As−S−Sb bridges, in accordance with the composition dependence of its relative intensity which was found to be maximum at $x = 0.5$.

1. Introduction

Chalcogenide glasses have attracted much attention over the years in light of their technological applications, including infrared-transmitting optical elements, xerography and lithography, acousto-optic and memory switching devices, and materials useful for image creation and storage.[1,2] In addition, chalcogenide glasses with enhanced ionic conductivity have been developed and found to exhibit properties suitable for electrochemical applications.[2−4]

$\mathrm{As_2S_3}$ is the most extensively studied chalcogenide glass mainly because of its ease of formation, its excellent infrared transmission and its resistance to atmospheric conditions and chemicals. Even though As and Sb belong to the same group of the periodic table, $\mathrm{As_2S_3}$ and $\mathrm{Sb_2S_3}$ do not display the same glass-forming tendency. Glassy $\mathrm{Sb_2S_3}$ is very difficult to form and its preparation requires high cooling rates.[5] However, addition of $\mathrm{As_2S_3}$ to $\mathrm{Sb_2S_3}$ enhances greatly the glass-forming ability of the latter and glasses in the mixed As−Sb−S system can be formed.[6]

It is generally accepted that the three-dimensional network of glassy $\mathrm{As_2S_3}$ is built of trigonal pyramidal units, $\mathrm{AsS_{3/2}}$, which are interconnected through As−S−As bridges.[5−10] There is also evidence that the intermediate range order of this glass involves two neighboring pyramids and their shared sulfur atom, with the correlation length being ∼7 Å.[11] The rearrangement of such coupled pyramids with respect to the neighbors has been proposed to explain properties such as reversible photoinduced structural changes.[11] Correspondingly, it has been shown that the basic structural units of glassy $\mathrm{Sb_2S_3}$ are the trigonal pyramids $\mathrm{SbS_{3/2}}$ bonded to each other by S atoms.[5,6] It is of interest to note that the resulting network of glassy $\mathrm{Sb_2S_3}$ exhibits a lower degree of local disorder around Sb atoms than that of crystalline $\mathrm{Sb_2S_3}$.[12]

Despite the general agreement on the glass structure of the two end members ($\mathrm{As_2S_3}$, $\mathrm{Sb_2S_3}$) the structure of glasses in the mixed system $\mathrm{Sb_2S_3}$−$\mathrm{As_2S_3}$ remains controversial. Early studies in this system were reported by Kawamoto and Tsuchihashi employing X-ray diffraction and infrared absorption spectroscopy.[6] They interpreted the results in terms of a microheterogeneous glass structure consisting of independent $\mathrm{As_2S_3}$ and $\mathrm{Sb_2S_3}$ regions, joined together by strained As−S−Sb linkages. The optical gap of glasses in the same system was studied by Tichy et al.[13] and found to change linearly with $\mathrm{Sb_2S_3}$ content. It was, therefore, suggested that the structure of such glasses can be considered as a nearly ideal solution of noninteracting $\mathrm{As_2S_3}$ and $\mathrm{Sb_2S_3}$ microphases. White et al.[14] investigated the crystallization kinetics of As−Sb−S glasses and found their results to be consistent with a heterogeneous structure of $\mathrm{As_2S_3}$ and $\mathrm{Sb_2S_3}$ phases. Raman and infrared spectra of glasses in the $\mathrm{Sb_2S_3}$−$\mathrm{As_2S_3}$ system were reported by Kato et al.[15] A two-mode behavior of the dominant modes originating from the intramolecular vibrations of $\mathrm{AsS_{3/2}}$ and $\mathrm{SbS_{3/2}}$ pyramidal units was observed, but no band characteristic of As−S−Sb bridges was resolved. Recent studies of As−Sb−S glasses by ^{121}Sb Mossbauer spectroscopy[16,17] and by the extended X-ray absorption fine structure (EXAFS) technique[18] support a different structural model. In particular, it was proposed that a random substitution of $\mathrm{AsS_{3/2}}$ by $\mathrm{SbS_{3/2}}$ pyramids takes place and leads to a homogeneous glass structure,[16−18] instead of the formation of two different microphases.

It is clear from the above that further work is required to help in resolving existing controversies concerning the structure of these mixed chalcogenide glasses. In this paper we present a systematic infrared reflectance study of glass compositions $x\mathrm{Sb_2S_3}\cdot(1-x)\mathrm{As_2S_3}$ in a wide glass forming region, $0 \le x \le 0.75$. The purpose of this investigation is twofold; first, to study the local glass structure as a function of composition and, second, to explore the possibility of formation of mixed As−S−Sb bridges.

* Corresponding author. Telephone: +30-1 724 9483. Fax: +30-1 724 9104. E-mail: eikam@eie.gr.

[⊗] Abstract published in *Advance ACS Abstracts,* November 15, 1997.

S1089-5647(97)02348-1 CCC: $14.00

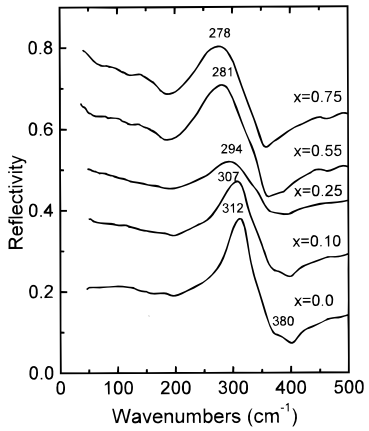

Figure 1. Infrared reflection spectra of $x\mathrm{Sb_2S_3}\cdot(1-x)\mathrm{As_2S_3}$ glasses. The spectra of glasses with $x = 0.10$, 0.25, 0.55, and 0.75 have been off-set by 0.175, 0.35, 0.45, and 0.5, respectively, to facilitate comparison.

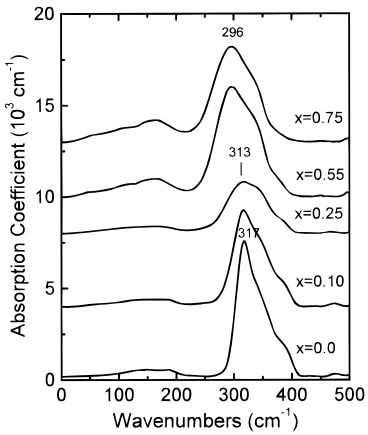

Figure 2. Absorption coefficient spectra of $x\mathrm{Sb_2S_3}\cdot(1-x)\mathrm{As_2S_3}$ glasses. Spectra of glasses with $0.1 \le x \le 0.75$ have been off-set to facilitate comparison.

2. Experimental Procedure

Glasses were prepared from stoichiometric mixtures of glassy $\mathrm{As_2S_3}$ and polycrystalline $\mathrm{Sb_2S_3}$. The starting materials were mixed and placed in silica ampules that were evacuated at about 10^{-5} Torr and sealed. Melting was performed at 850 °C for ca. 8 h in a rotating furnace in order to ensure homogeneity of the melt. Glasses were then obtained by water-quenching the silica tubes. This technique results in $x\mathrm{As_2S_3}\cdot(1-x)\mathrm{Sb_2S_3}$ glasses with compositions spanning a wide and continuous glass forming region, $0 \le x \le 0.75$. The color of the glasses obtained varies from red to dark red upon increasing $\mathrm{Sb_2S_3}$ content. The bulk glasses were cut using a low speed diamond saw and polished to yield flat samples with good quality surfaces appropriate for infrared reflectance measurements.

Infrared spectra were recorded in the reflectance mode at near normal incidence (11° off-normal) on a Fourier-transform vacuum spectrometer (Bruker 113v), using a high reflectivity Al mirror as reference. A Hg source, a DTGS detector with polyethylene window and five Mylar beam splitters with variable thickness (3.5−50 μm) were used in the far-infrared region in order to measure continuous spectra in the range 30−700 $\mathrm{cm^{-1}}$. Each spectrum represents the average of 200 scans with 2 $\mathrm{cm^{-1}}$ resolution. The measured reflectivity spectra were analyzed by the Kramers−Kronig inversion technique to obtain the absorption coefficient spectra, as described in details elsewhere.[19,20]

3. Results

Figure 1 presents infrared reflectance spectra of $x\mathrm{Sb_2S_3}\cdot(1-x)\mathrm{As_2S_3}$ glasses with $\mathrm{Sb_2S_3}$ contents spanning the entire glass forming region. The measured reflectivity spectra are in good agreement with those reported earlier by Kato et al. in the composition range $0 \le x \le 0.60$.[15] The spectrum of pure $\mathrm{As_2S_3}$ glass ($x = 0$) is characterized by a strong reflection band at 312 $\mathrm{cm^{-1}}$, a weak band at 380 $\mathrm{cm^{-1}}$ and a very weak feature in the range 50−150 $\mathrm{cm^{-1}}$. Addition of $\mathrm{Sb_2S_3}$ to $\mathrm{As_2S_3}$ induces systematic spectral changes. Thus, increasing x results in the broadening of the main reflection band and its shifting to lower frequencies (278 $\mathrm{cm^{-1}}$ for $x = 0.75$), followed by the progressive weakening of the 380 $\mathrm{cm^{-1}}$ feature.

Corresponding changes are observed also in the absorption coefficient spectra of these glasses displayed in Figure 2. The dominant high-frequency absorption profile (250−450 $\mathrm{cm^{-1}}$) becomes broader and shifts to lower frequencies upon increasing $\mathrm{Sb_2S_3}$ content. Also, the absorption envelope below 200 $\mathrm{cm^{-1}}$ acquires intensity as x increases and peaks eventually at ca. 160 $\mathrm{cm^{-1}}$ for $x = 0.75$.

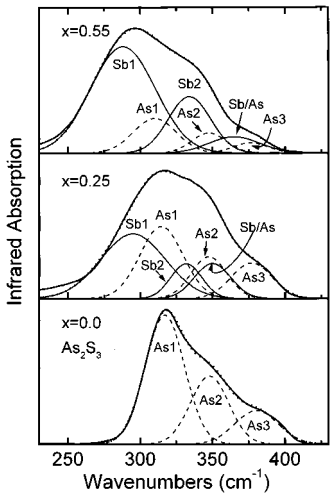

Figure 3. Examples of deconvolution of the higher-frequency envelope (250−450 $\mathrm{cm^{-1}}$) of the infrared spectra of $x\mathrm{Sb_2S_3}\cdot(1-x)\mathrm{As_2S_3}$ glasses. Experimental spectra are shown by thick continuous lines, component bands are shown by dashed lines and thin continuous lines, and simulated spectra are shown by dotted lines.

To understand the structural origin of these spectral changes, further analysis of the infrared spectra is required. In particular, we focus attention on revealing the structures responsible for the evolution of the complex profile from 250 to 450 $\mathrm{cm^{-1}}$, since absorption due to stretching vibrations of As−S and Sb−S bonds is expected in this frequency range. Thus, we have attempted to deconvolute this high frequency envelope, to assign the resulting component bands and to understand the composition dependence of their relative intensities. For this purpose we apply a nonlinear least-squares fitting program and a deconvolution procedure employed previously to study binary and ternary glasses.[19−21] The basis of our approach is to use the minimum number of component bands that gives a reasonable agreement between experimental and calculated spectra. The functional form, the frequencies, bandwidths and intensities of component bands are parameters adjustable by the program. The steps followed in this work for spectral deconvolution are described below.

We have started spectral analysis by considering first the high-frequency absorption envelope of the $\mathrm{As_2S_3}$ glass ($x = 0$), shown in Figure 3 in an expanded frequency scale. The profile of the 250−450 $\mathrm{cm^{-1}}$ envelope for this glass suggests the existence of at least three component bands. Indeed, a good fit was obtained with three bands of Gaussian line shape as shown in Figure 3. The three components, designated by As1, As2, and

As3, have their peaks at frequencies 317, 348, and 380 cm^{-1}, respectively. The assignment of these bands can be made on the basis of the molecular model proposed by Lucovsky and Martin[7] for the interpretation of the vibrational spectra of chalcogenide glasses As_2X_3 (X = S, Se, Te). This model was found useful to treat the vibrational spectra of analogous oxide glasses such as As_2O_3,[22] as well as those of binary chalcogenide glasses, like $Li_2S-As_2S_3$.[23] According to this model, the vibrational features of glass are attributed to intramolecular vibrations of $AsX_{3/2}$ pyramids and As−X−As water-like molecules, which are assumed to be vibrationally decoupled.[7] Therefore, the strongest infrared band of As_2S_3 deconvoluted at 317 cm^{-1} (As1) can be assigned to the asymmetric stretching mode, ν_3(E), of the $AsS_{3/2}$ pyramid, while the one at 348 cm^{-1} (As2) to the symmetric stretching mode, $\nu_1(A_1)$, of the same unit.[8] Besides these modes, $AsS_{3/2}$ pyramids exhibit two bending modes, ν_4(E) and $\nu_2(A_1)$, which are also infrared active and contribute to the weak absorption in the 100−200 cm^{-1} frequency range (Figure 2). The high-frequency component deconvoluted at 380 cm^{-1} (As3) is attributed to the asymmetric stretching vibration of As−S−As bridges, ν_{as}(As−S−As). The above assignments are consistent with the Raman spectrum of glassy As_2S_3 which exhibits strong scattering at 343 cm^{-1} (ν_1), a weaker feature at 312 cm^{-1} (ν_3) and a shoulder at 373 cm^{-1} (ν_{as}(As−S−As)).[9]

Infrared spectra of glassy Sb_2S_3 prepared in various forms have been reported by several authors.[24−26] According to Poltavcev et al.[24] the IR spectrum of amorphous Sb_2S_3 film shows the strongest band at 275 cm^{-1} due to the ν_3 mode of $SbS_{3/2}$ pyramids, in analogy with As_2S_3 glass. Droichi et al.[25] measured strong infrared absorption for glassy Sb_2S_3 films at 285 cm^{-1} for the ν_3 mode, and a weaker feature at 330 cm^{-1} which was not assigned. Bernier et al.[26] reported bands of amorphous Sb_2S_3 dispersed in paraffin at 293 and 332 cm^{-1}, and assigned them to the ν_3 and ν_1 modes of $SbS_{3/2}$ pyramids, respectively. Kato et al.[15] obtained by extrapolation the ν_3 mode of glassy Sb_2S_3 at 270 cm^{-1} and the ν_1 mode at 297 cm^{-1}, while Giehler reported ν_1 at 304 cm^{-1}.[9] It is clear that even though there is no agreement in the literature for the exact position and assignments of the infrared active bands of glassy Sb_2S_3, its spectrum is characterized by the presence of two bands; one in the range ∼270−290 cm^{-1} and the second in the range ∼300−335 cm^{-1}.

With the above information in mind, and on the basis of the results of deconvolution of the spectrum of As_2S_3 ($x = 0$), we deconvoluted the spectra of mixed $Sb_2S_3-As_2S_3$ glasses ($x > 0$). As input we used the frequencies and bandwidths of bands As1, As2, and As3 as determined for $x = 0$, and two additional bands at ca. 280 and 325 cm^{-1} to account for the presence of the Sb_2S_3 component in the mixed glass. With these five component bands we could fit the 250−450 cm^{-1} spectral profile quite satisfactorily. Using this approach, we found that in all cases the intensity of the As2 band is equal or even higher than that of the As1 component. However, there is no reason to believe that the symmetric stretching mode of the $AsS_{3/2}$ pyramid, ν_1(As2), which is the strongest Raman band of the As_2S_3 glass,[9] acquires additional intensity in the infrared spectra of the mixed glasses. Therefore, we take this finding as suggesting the presence of an additional component close to the As2 band. Consequently, the spectra of mixed glasses were fitted with the input presented above and the consideration of a sixth component at ca. 360 cm^{-1}. In this way, the relative intensities of the resulting As1 and As2 components were found similar to that in the spectrum of the $x = 0$ glass. Typical results of deconvolution are shown in Figure 3, where the additional components in the spectra of mixed glasses at ca. 280, 330, and 360 cm^{-1} are marked by Sb1, Sb2, and Sb/As, respectively. The frequencies of the resulting component bands are plotted in Figure 4 versus mole fraction of Sb_2S_3.

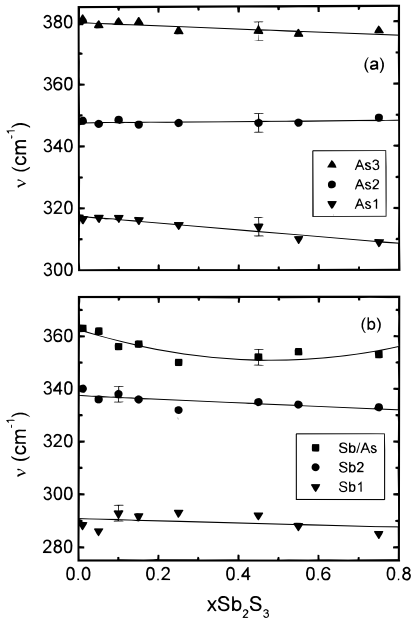

Figure 4. Composition dependence of the frequencies of the component bands resulted from the deconvolution of the 250−450 cm^{-1} absorption envelope of $xSb_2S_3 \cdot (1-x)As_2S_3$ glasses. Lines are least-squares fittings to the data.

4. Discussion

4.1. Infrared Band Assignments. According to the molecular model[7] and in analogy with glassy As_2S_3, we assign the As1, As2, and As3 components in the deconvoluted spectra of mixed glasses to the $\nu_3(AsS_{3/2})$, $\nu_1(AsS_{3/2})$, and ν_{as}(As−S−As) modes, respectively. As shown in Figure 4a the frequencies of these modes vary linearly with Sb_2S_3 concentration but they do not display a large variation with composition, suggesting that the structure of the basic building units, i.e., $AsS_{3/2}$ pyramids and As−S−As bridges, is retained in the mixed glasses. Nevertheless, the frequency trends observed in Figure 4a deserve our attention. In particular, we note that the difference ν_1(As2) − ν_3(As1) increases with x, while the frequency of the As3 band decreases with Sb_2S_3 content.

To search for the origin of these frequency trends we consider first the ν_1 and ν_3 modes of $AsS_{3/2}$ pyramid. General expressions for the frequencies of the vibrational modes of an XY_3 pyramid were obtained originally by Herzberg on the basis of the valence force field model.[27] The expressions for ν_1 and ν_3 modes were simplified by Lucovsky[28] by assuming negligible displacement of Y atoms for the stretching modes:

$$\nu^2_1 = (1/(4\pi^2c^2))(3k_r/m_X)\,[\cos^2\beta + 12\gamma\cos^2\beta \times \sin^2\beta/(1+3\cos^2\beta)] \quad (1)$$

$$\nu^2_3 = (1/(4\pi^2c^2))\,(3k_r/(2m_X))[\sin^2\beta + 3\gamma\sin^4\beta/(1+3\cos^2\beta)] \quad (2)$$

where c is the speed of light, m_X is the mass of atom X, k_r is the stretching force constant of bond X−Y, γ is defined by $\gamma = k_\phi/k_r$ with k_ϕ being the Y−X−Y bond bending force constant, and β is the angle between the X−Y bond and the 3-fold symmetry axis of the pyramid (see Figure 5). The angle β is related to the Y−X−Y bond angle (ϕ) by the expression

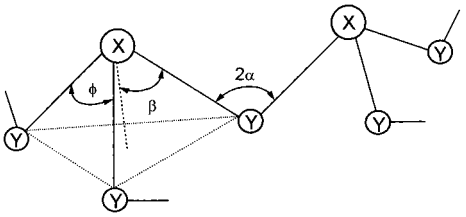

Figure 5. Schematic diagram of the local order in an X_2Y_3 chalcogenide glass (X = As, Sb, Y = S).

$$\sin\beta = 2\sin(\phi/2)/\sqrt{3} \qquad (3)$$

According to Cervinka and Hruby[5] the S−As−S bonding angle in glassy As_2S_3 is $\phi = 102.3°$ which results in $\beta = 64°$-(eq 3), while Lucovsky suggested that $\beta = 60°$.[8] We employ an average value of $\beta = 62°$, and the frequency values $\nu_1 = 348\ cm^{-1}$ and $\nu_3 = 317\ cm^{-1}$ as determined by spectral deconvolution, to obtain the values of k_r and γ for the $AsS_{3/2}$ pyramid. Application of eqs 1 and 2 results in $k_r = 2.36 \times 10^5$ dyn/cm and $\gamma = 0.43$. In Figure 6 we examine the dependence of $\nu_3(AsS_{3/2})$ and $\nu_1(AsS_{3/2})$ on β, k_r and γ in order to understand the composition dependence of ν_3 and ν_1 in mixed Sb_2S_3−As_2S_3 glasses. It is clear that the difference between the symmetric and asymmetric stretching modes of the $AsS_{3/2}$ pyramid is affected mostly by angle β (Figure 6a). To explore further this effect, we plot in Figure 7 the calculated difference $\nu_1 - \nu_3$ versus β for values close to 62°, and compare with the experimentally determined frequency differences. As shown in Figure 7, the experimental $\nu_1 - \nu_3$ difference increases with Sb_2S_3 content. This increase of $\nu_1 - \nu_3$ results in a decrease of β by ∼1° from $x = 0$ to $x = 0.75$, and this corresponds according to eq 3 to a decrease of the S−As−S angle by ∼1° also.

We consider now the composition dependence of the frequency of the As3 band. The frequency of the asymmetric stretching mode of X−Y−X bridges, ν_{as}(X−Y−X), is given by the simplified expression

$$\nu^2_{as} = (1/(4\pi^2c^2))(2k_r/m_Y)\sin^2\alpha \qquad (4)$$

where m_Y is the mass of atom Y, k_r is the force constant of bond X−Y, and 2α is the X−Y-X bond angle.[28] The As−S−As bond angle in As_2S_3 glass was estimated to be $2\alpha = 99.5°$,[5] while the As−S force constant was determined above to be $k_r = 2.36 \times 10^5$ dyn/cm. Consideration of these values and application of eq 4 give ν_{as}(As−S−As) = 382 cm^{-1}, in very good agreement with the experimental value (380 cm^{-1} for $x = 0$). Assuming now that the force constant of the As−S bond is less sensitive to addition of Sb_2S_3 than the As−S−As bond angle, the decrease of ν_{as}(As−S−As) with increasing x (see Figure 4a) suggests a decrease of the bridging bond angle (2α). For small changes in α, we can obtain Δ(2α) in terms of $\Delta\nu_{as}$ by differentiating eq 4 as follows:

$$\Delta(2\alpha) = (4\pi^2c^2)(m_Y\,\nu_{as}/(k_r\sin\alpha\cos\alpha))\Delta\nu_{as} \qquad (5)$$

For a frequency decrease $\Delta\nu_{as} \approx 5\ cm^{-1}$ from $x = 0$ to $x = 0.75$ (Figure 4a) eq 5 gives $\Delta(2\alpha) \approx 2°$. Therefore, application of the molecular model to the vibrational modes characterizing As−S bonding in mixed As−Sb−S glasses leads to the conclusion that the pyramidal (S−As−S) and the bridging bond (As−S−As) angles decrease by ∼1° and 2°, respectively, as the Sb_2S_3 content varies in the range $0 \le x \le 0.75$.

It would be desirable to apply the same procedure for Sb−S bonding in these glasses; however, this cannot be done because of the lack of agreement on the frequency values for the ν_1 and ν_3 modes of glassy Sb_2S_3 ($x = 1$). In an alternative approach, we can use the following scaling expression[9] to obtain the stretching force constant, k_r(Sb−S), of the Sb−S bond:

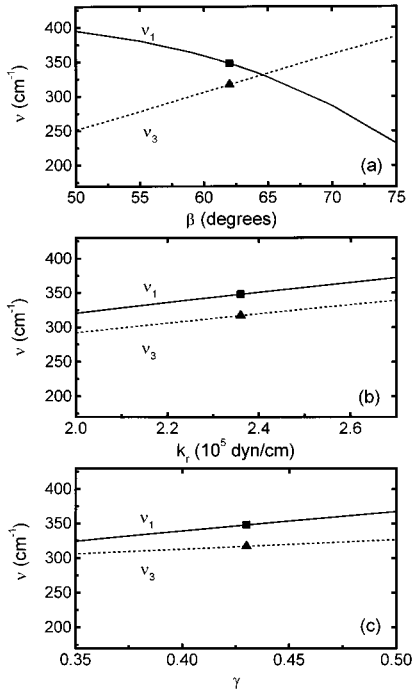

Figure 6. Frequencies of the stretching modes (ν_1 and ν_3) of the $AsS_{3/2}$ pyramid calculated by means of eqs 1 and 2 as a function of (a) the pyramidal angle β, with $k_r = 2.36 \times 10^5$ dyn/cm and $\gamma = 0.43$, (b) the stretching force constant of the As−S bond, k_r, with $\beta = 62°$ and $\gamma = 0.43$, and (c) the bond bending to bond stretching force constant ratio, γ, with $k_r = 2.36 \times 10^5$ dyn/cm and $\beta = 62°$. The values of ν_1 and ν_3 for $AsS_{3/2}$ pyramid obtained in this work by deconvoluting the spectrum of glassy As_2S_3 (see Figure 3) are marked by squares and triangles, respectively.

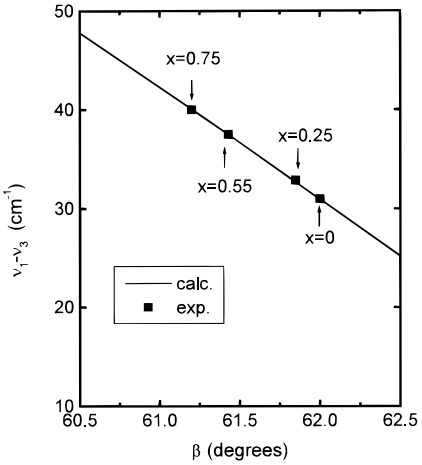

Figure 7. Frequency difference of the symmetric (ν_1) and asymmetric (ν_3) stretching modes of the $AsS_{3/2}$ pyramid versus the pyramidal angle β calculated by means of eqs 1 and 2, with $k_r = 2.36 \times 10^5$ dyn/cm and $\gamma = 0.43$. Data points mark experimental frequency differences for representative glass compositions in the system $x Sb_2S_3 \cdot (1 - x)$-As_2S_3.

$$k_r(Sb{-}S) = k_r(As{-}S)d^3_{As-S}/d^3_{Sb-S} \qquad (6)$$

where k_r(As−S) = 2.36×10^5 dyn/cm, and the bond lengths, $d_{As(Sb)-S}$, are taken as the sum of the covalent radii of the bond forming atoms, i.e., $d_{As-S} = 2.24$ Å and $d_{Sbs-S} = 2.45$ Å.[29] From eq 6 we get k_r(Sb−S) = 1.80×10^5 dyn/cm, and since the Sb−S−Sb bond angle in glassy Sb_2S_3 has been estimated

($2\alpha = 100.7°$ [5]) we may apply eq 4 to obtain the frequency of the asymmetric stretching mode of Sb−S−Sb bridges. The result is ν_{as}(Sb−S−Sb) = 336 cm^{-1}, suggesting that the band measured at ca. 330 cm^{-1} in the infrared spectrum of glassy Sb_2S_3,[25,26] as well as the Sb2 band deconvoluted in the spectra of mixed As−Sb−S glasses (Figure 4b), result from the overlap of the ν_1($SbS_{3/2}$) and ν_{as}(Sb−S−Sb) modes. The Sb1 band deconvoluted at ca. 290 cm^{-1} (Figure 4b) can be safely attributed to the ν_3 mode of $SbS_{3/2}$ pyramidal units. It is of interest to note that a linear fit of the frequency data related to Sb−S bonding in Figure 4b and extrapolation to $x = 1.0$ give Sb1 at 287 cm^{-1} and Sb2 at 331 cm^{-1}, in excellent agreement with the frequencies of the main bands in the infrared spectrum of amorphous Sb_2S_3 film.[25]

The deconvoluted component which has not been assigned so far is the one designated by Sb/As in Figure 3. The frequency of this band varies slightly nonlinearly with x as shown in Figure 4b, and is found to be between those obtained for the asymmetric stretching modes of pure As−S−As (382 cm^{-1}) and pure Sb−S−Sb (336 cm^{-1}) bridges. This suggests that the Sb/As band can be assigned to the ν_{as} mode of mixed As−S−Sb bridges. To check the validity of this assignment, we employ eq 4 to estimate ν_{as}(As−S−Sb). For the sake of simplicity, the required values for an effective stretching force constant and for the As−S−Sb bond angle are set equal to the average values of the corresponding quantities for As−S−As and Sb−S−Sb bridges in the two end members, i.e., $k_{av} = 2.08 \times 10^5$ dyn/cm and $2\alpha_{av} = 100.1°$. The calculated frequency, ν_{as}(As−S−Sb) = 360 cm^{-1}, is in good agreement with the average experimental frequency of the Sb/As band (358 cm^{-1}). This lends support to the above assignment and strongly suggests the formation of mixed As−S−Sb bridges in these glasses. The nonlinear variation of ν_{as}(As−S−Sb) with x can result from the combined effect of the force constant and of the As−S−Sb bond angle (eq 4), both of which may vary with composition.

4.2. Composition Dependence of Relative Intensities: Heterogeneous Phases or Random Substitution? In this section we study the composition dependence of the deconvoluted infrared bands with the purpose of gaining more insight into the nature of these chalcogenide glasses. The salient feature of the deconvoluted spectra of As−Sb−S glasses is the identification of the band due to As−S−Sb bridges (Sb/As), besides those characterizing bonding similar to that in the two end member components. In particular, the structure related to As−S bonding is characterized by $AsS_{3/2}$ pyramids (bands As1 and As2) and As−S−As bridges (band As3), while for $SbS_{3/2}$ pyramids the ν_3 mode is correlated with band Sb1, but the ν_1 mode was found to overlap with the ν_{as} mode of Sb−S−Sb bridges (band Sb2). To separate the contribution of ν_1 and ν_{as} modes of Sb−S bonding and calculate relative intensities, we note that for As−S bonding the As3 component constitutes approximately 35% of the total intensity of bands As2 and As3. Assuming that an analogous situation holds for Sb−S bonding, we attribute 35% of the intensity of band Sb2 to the ν_{as}(Sb−S−Sb) mode and 65% to the ν_1($SbS_{3/2}$) mode. On these grounds, we could calculate separately the relative intensity of bands characterizing pyramidal units ($AsS_{3/2}$, $SbS_{3/2}$), and those related to bridging bonds (As−S−As, As−S−Sb). The results are shown in Figures 8 and 9 as a function of Sb_2S_3 content, noting that relative intensities were obtained by normalizing with the sum of the intensities of the type of modes considered in each case.

The intensities of bands attributed to modes ν_3($AsS_{3/2}$) and ν_1($AsS_{3/2}$), as well as those of ν_3($SbS_{3/2}$) and ν_1($SbS_{3/2}$) modes, have been considered together in Figure 8 because they originate

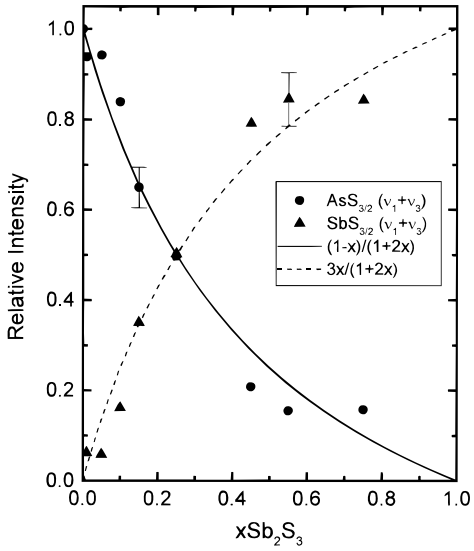

Figure 8. Composition dependence of experimental (data points) and calculated (lines) relative intensities of bands assigned to the symmetric (ν_1) and asymmetric (ν_3) stretching modes of $AsS_{3/2}$ and $SbS_{3/2}$ pyramidal units in $x$$Sb_2S_3$·$(1 - x)$$As_2S_3$ glasses. For details see text.

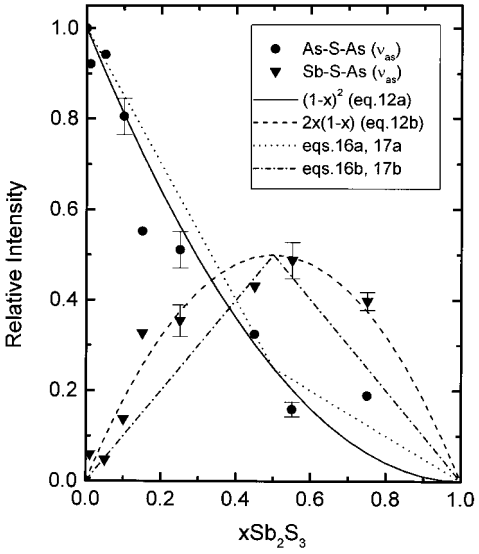

Figure 9. Composition dependence of experimental (data points) and calculated (lines) relative intensities of bands assigned to the asymmetric stretching modes (ν_{as}) of As−S−As and Sb−S−As bridging bonds in $x$$Sb_2S_3$·$(1 - x)$$As_2S_3$ glasses. For details see text.

from intramolecular vibrations of the $XS_{3/2}$ pyramids (X = As, Sb). It is found that the relative intensity of bands due to $AsS_{3/2}$ pyramids decreases monotonically with Sb_2S_3 content, while the relative intensity of bands assigned to $SbS_{3/2}$ pyramids increases with x as expected. It is noted though that the infrared activity of $SbS_{3/2}$ pyramids is considerably higher than would be expected from the mole fraction of Sb_2S_3 alone. To explain these findings, we write the relative intensity of bands assigned to pyramids as follows:

$$I_{AsS3/2} = (1 - x)\alpha_{AsS3/2}/[x\alpha_{SbS3/2} + (1 - x)\alpha_{AsS3/2}] \quad (7a)$$

$$I_{SbS3/2} = x\alpha_{SbS3/2}/[x\alpha_{SbS3/2} + (1 - x)\alpha_{AsS3/2}] \quad (7b)$$

where $\alpha_{AsS3/2}$ and $\alpha_{SbS3/2}$ are effective absorption coefficients of the ν_3 and ν_1 modes of $AsS_{3/2}$ and $SbS_{3/2}$ pyramids, respectively. Since the values of $\alpha_{AsS3/2}$ and $\alpha_{SbS3/2}$ are not known we proceed by defining a relative absorption coefficient $\alpha_{rel} = \alpha_{SbS3/2}/\alpha_{AsS3/2}$ and rewriting eqs 7 in the form

$$I_{AsS3/2} = (1 - x)/[1 + (\alpha_{rel} - 1)x] \quad (8a)$$

$$I_{SbS3/2} = x\alpha_{rel}/[1 + (\alpha_{rel} - 1)x] \quad (8b)$$

The best fit of eq 8a and 8b to the experimental data was obtained with $\alpha_{rel} = 3$ (Figure 8), suggesting that the Sb−S oscillator is approximately three times stronger infrared absorber than the As−S oscillator. This is in agreement with previous findings that the effective charge involved in the Sb−S bonding is considerably higher than that involved in As−S bonding.[9,15]

The relative intensity of band As3 is found to decrease monotonically with x (Figure 9), indicating the progressive destruction of As−S−As bridges as the As_2S_3 content in the mixed glass decreases. The relative intensity of band Sb/As displays a nonlinear dependence on x, passing through a maximum value at $x \approx 0.5$ (Figure 9). Since the probability for creating mixed Sb−S−As bridges would be maximized at $x = 0.5$, the composition dependence of the relative intensity of the Sb/As band is consistent with its assignment to ν_{as}(Sb−S−As).

In Figure 9 we compare also the experimental relative intensities attributed to bridging bonds with those calculated on the basis of the models proposed for the structure of the As−Sb−S glasses. We write these relative intensities in the form

$$I_{As-S-As} = f_{As-S-As}\alpha_{As-S-As}/\sum f_i\alpha_i \quad (9a)$$

$$I_{Sb-S-As} = f_{Sb-S-As}\alpha_{Sb-S-As}/\sum f_i\alpha_i \quad (9b)$$

where

$$\sum f_i\alpha_i = f_{As-S-As}\alpha_{As-S-As} + f_{Sb-S-Sb}\alpha_{Sb-S-Sb} + f_{Sb-S-As}\alpha_{Sb-S-As} \quad (9c)$$

with f_{X-S-X} denoting the fraction of bridges X−S−X (X = As and/or Sb) and α_{X-S-X} being the absorption coefficient of the asymmetric stretching mode of the bridging bond. Since this particular vibrational mode involves mainly the displacement of the bridging S atom (eq 4, and ref 28) we may set $\alpha_{As-S-As} \approx \alpha_{Sb-S-Sb} \approx \alpha_{Sb-S-As}$. This approximation simplifies the above equations as follows:

$$I_{As-S-As} = f_{As-S-As}/\sum f_i \quad (10a)$$

$$I_{Sb-S-As} = f_{Sb-S-As}/\sum f_i \quad (10b)$$

The fractions of the three type of bridging bonds are now calculated in terms of the two structural models proposed in the literature: (a) random substitution of As by Sb [16−18] and (b) formation of heterogeneous As_2S_3 and Sb_2S_3 microphases, which could be connected at their interfaces via mixed Sb−S−As bridges.[6,13−15] In both cases, it is assumed that As and Sb are 3-fold coordinated to S atoms only, and that each S atom is 2-fold coordinated to As and/or Sb atoms.

It can be easily shown that for the random substitution model the fractions of three center linkages are given by

$$f_{As-S-As} = (1 - x)^2 \quad (11a)$$

$$f_{Sb-S-As} = 2x(1 - x) \quad (11b)$$

$$f_{Sb-S-Sb} = x^2 \quad (11c)$$

and thus the relative intensities of interest become:

$$I_{As-S-As} = (1 - x)^2 \quad (12a)$$

$$I_{Sb-S-As} = 2x(1 - x) \quad (12b)$$

Relative intensities calculated according to eqs 12a and 12b are compared in Figure 9 with the experimental data. The agreement between experiment and calculation based on the random substitution model is quite good.

Let us now consider the heterogeneous As_2S_3/Sb_2S_3 microphase model and suppose that mixed Sb−S−As bridges are formed at the interfaces according to the reaction

$$As-S-As + Sb-S-Sb \rightarrow 2\,(Sb-S-As) \quad (13)$$

If we call p the probability that the above reaction takes place at the interface of the two different microphases, then it can be shown that the fractions of bridging bonds are given by the equations

for $0 \le x \le 0.5$

$$f_{As-S-As} = (1 - x) - px \quad (14a)$$

$$f_{Sb-S-As} = 2px \quad (14b)$$

$$f_{Sb-S-Sb} = x(1 - p) \quad (14c)$$

for $0.5 \le x \le 1$

$$f_{As-S-As} = (1 - x)(1 - p) \quad (15a)$$

$$f_{Sb-S-As} = 2p(1 - x) \quad (15b)$$

$$f_{Sb-S-Sb} = x - p(1 - x) \quad (15c)$$

Equations 10a, 10b are now rearranged in terms of eqs 14 and 15 to give the relative intensities of interest in the two composition ranges:

for $0 \le x \le 0.5$

$$I_{As-S-As} = (1 - x) - px \quad (16a)$$

$$I_{Sb-S-As} = 2px \quad (16b)$$

for $0.5 \le x \le 1$

$$I_{As-S-As} = (1 - x)(1 - p) \quad (17a)$$

$$I_{Sb-S-As} = 2p(1 - x) \quad (17b)$$

We found that the best fit of eqs 16a, 16b and 17a, 17b to the experimental data is obtained for $p = 0.5$ (see Figure 9). Comparison of the results given by the two models shows that the random substitution model gives a better agreement with the experimental relative intensity data. Further evidence in favor of this model is provided by the frequency data discussed in the previous section. If heterogeneous As_2S_3 and Sb_2S_3 microphases were formed, one would expect that at least the intramolecular vibrations of $XS_{3/2}$ pyramids in the two different microphases would be independent of composition. However, this was not observed in the present work. In particular, the systematic variation with Sb_2S_3 content especially of the ν_1 and

ν_3 modes of $AsS_{3/2}$ pyramids is indicating considerable neighboring of the $AsS_{3/2}$ and $SbS_{3/2}$ structural units.

5. Conclusions

Chalcogenide glasses in the mixed system $xSb_2S_3\cdot(1-x)$-As_2S_3 have been prepared in a wide composition range ($0 \leq x \leq 0.75$) and their structure was investigated by infrared reflectance spectroscopy. The high-frequency profiles (250−450 cm^{-1}) of the absorption coefficient spectra were deconvoluted into component bands in order to study the composition dependence of glass structure. The main components of the deconvoluted high-frequency spectra were understood on the basis of the asymmetric and symmetric stretching vibrational modes of trigonal $AsS_{3/2}$ and $SbS_{3/2}$ pyramids. While the structure of the pyramidal units is retained in the mixed glasses, it was found that the pyramidal S−As−S angle, and the bridging As−S−As angle decrease by approximately 1° and 2°, respectively, as x increases from 0 to 0.75. Besides bands due to the intramolecular modes of pyramids, a band was resolved at ca. 380 cm^{-1} and was attributed to the asymmetric stretching mode of As−S−As bridges in accordance with the molecular model. The frequency of the analogous mode of Sb−S−Sb bridges was calculated to be close to that of the symmetric stretching mode of $SbS_{3/2}$ pyramids (ca. 330 cm^{-1}).

The salient feature of this study is the identification of a band deconvoluted at ca. 360 cm^{-1} with mixed Sb−S−As bridges. The destruction of As−S−As bridges with increasing Sb_2S_3 content was found to be accompanied by the creation of mixed Sb−S−As bridges, with the relative abundance of the latter bridges showing its maximum value at ca. $x = 0.5$. The experimental relative intensities were compared with those calculated on the basis of the random substitution and heterogeneous structure models. It was found that both the frequency and relative intensity data are suggestive of a considerable mixing of $AsS_{3/2}$ and $SbS_3/2$ pyramidal units, rather than of the formation of separate As_2S_3 and Sb_2S_3 microphases connected at the interfaces.

Acknowledgment. This work was supported in part by the NATO Special Fellowships Program and by NHRF. Two of us (E.I.K, J.A.K) are very grateful to Dr. C. P. Varsamis for his help with spectral deconvolution.

References and Notes

(1) Seddon, A. B. *J. Non-Cryst. Solids* **1995**, *184*, 44.
(2) Elliott, S. R. In *Materials Science and Technology. Glasses and Amorphous Materials*, Zarzycki, J. Ed.; VCH: Weinheim, 1991, vol. 9, pp 375−454.
(3) Souquet, J. L.; Robinel, E.; Barrau, B.; Ribes, M. *Solid State Ionics* **1981**, *3*−*4*, 317.
(4) Reau, J. M.; Tanguy, B.; Videau, J. J.; Portier, J.; Hagenmuller, P. *Solid State Ionics* **1988**, *28*−*30*, 792.
(5) Cervinka, L.; Hruby, A. *J. Non-Cryst. Solids* **1982**, *48*, 231.
(6) Kawamoto, Y.; Tsuchihashi, S. *Yogyo-Kyokai-Shi* **1969**, *77*, 328.
(7) Lucovsky, G.; Martin, R. *J. Non-Cryst. Solids* **1972**, *8*−*10*, 185.
(8) Lucovsky, G. *Phys. Rev. B* **1971**, *6*, 1480.
(9) Giehler, M. *Phys. Status Solidi. B* **1981**, *106*, 193.
(10) Itoh, S.; Fujiwara, T. *J. Non-Cryst. Solids* **1982**, *51*, 175.
(11) Paesler, M. A.; Pfeiffer, G. *J. Non-Cryst. Solids* **1991**, *137*−*138*, 967.
(12) Dalba, G.; Fornasini, P.; Giunta, G.; Burattini, E. *J. Non-Cryst. Solids* **1989**, *107*, 261.
(13) Tichy, L.; Triska, A.; Frumar, M.; Ticha, H.; Klikorka, J. *J. Non-Cryst. Solids* **1982**, *50*, 371.
(14) White, K.; Crane, R. L.; Snide, J. A. *J. Non-Cryst. Solids* **1988**, *103*, 210.
(15) Kato, M.; Onari, S.; Arai, T. *Jpn. J. Appl. Phys*. **1983**, *22*, 1382.
(16) Bychkov, E.; Wortmann, G. *J. Non-Cryst. Solids* **1993**, *159*, 162.
(17) El Idrissi Raghni, M. A.; Lippens, P. E.; Olivier-Fourcade, J.; Jumas, J. C. *J. Non-Cryst. Solids* **1995**, *192*−*193*, 191.
(18) Durand, J. M.; Lippens, P. E.; Olivier-Fourcade, J.; Jumas, J. C. *J. Non-Cryst. Solids* **1995**, *192*−*193*, 364.
(19) Kamitsos, E. I.; Patsis, A. P.; Karakassides, M. A.; Chryssikos, G. D. *J. Non-Cryst. Solids* **1990**, *126*, 52.
(20) Kamitsos, E. I.; Yiannopoulos, Y. D.; Karakassides, M. A.; Chryssikos, G. D.; Jain, H. *J. Phys. Chem.* **1996**, *100*, 11755.
(21) Kamitsos, E. I.; Yiannopoulos, Y. D.; Jain, H.; Huang, W. C. *Phys. Rev. B* **1996**, *54*, 9775.
(22) Papatheodorou, G. N.; Solin, S. A. *Solid State Commun*. **1975**, *16*, 5.
(23) Shastry, M. C.R.; Couzi, M.; Levasseur, A.; Menetrier, M. *Philos. Mag. B* **1993**, *68*, 551.
(24) Poltavcev, J. G.; Zacharov, B. P.; Gerasimenko, V. S.; Kucerenko, L. P. *Izv. Akad. Nauk. SSSR, Neorg. Mater.* **1974**, *10*, 367.
(25) Droichi, M. S.; Vaillant, F.; Bustarret, E.; Jousse, D. *J. Non-Cryst. Solids* **1988**, *101*, 151.
(26) Barnier, S.; Guittard, M.; Julien, C.; Chilouet, A. *Mater. Res. Bull.* **1993**, *28*, 399.
(27) Herzberg, G. *Infrared and Raman Spectra of Polyatomic Molecules*; Van Nostrand: New York, 1945; Chapter II, pp 148−154.
(28) Lucovsky, G. *Philos. Mag. B* **1979**, *39*, 513.
(29) Huheey, J. E. *Inorganic Chemistry, Principles of Structure and Reactivity*, 2nd ed.; Harper & Row: London, 1978; p 232.